Imaging of alkyne-functionalized ruthenium complexes for photoactivated chemotherapy

Busemann, A.

5

SYNTHESIS OF OTHER ALKYNE-FUNCTIONALIZED RUTHENIUM POLYPYRIDYL COMPLEXES

The synthesis of three alkyne-functionalized polypyridyl complexes is reported. The complex [Ru(RCC-tpy)(bpy)(MTI-SRR')]$(PF_6)_2$, where MTI-SRR' = a thioether-rigidin conjugate, RCC-tpy = 4'-(tert-butyldimethylsilyl)-2,2':6',2''-terpyridyne, and bpy = 2,2'-bipyridine, was synthesized starting from an acetonitrile precursor. The reaction resulted in the formation of a reaction mixture. The complex [Ru(Ph_2phen)(mtmp)(RCC-bpy)]$(PF_6)_2$, where Ph_2phen = 4,7-diphenyl-1,10-phenantroline, mtmp = 2-(methylthio)methylpyridine, and RCC-bpy = 4'-(tert-butyldimethylsilyl)-2,2'-bipyridine, was synthesized starting from the known acetonitrile precursor [Ru(Ph_2phen)(mtmp)$(MeCN)_2$]$(PF_6)_2$. Despite the potentially increased reactivity due to the presence of two cis coordination positions on the metal center during coordination of the alkyne-functionalized bipyridine ligand, the desired complex was isolated in good yield as a mixture of two diastereoisomers. Reaction of [Ru$(DMSO)_4(Cl)_2$] with alkyne-functionalized H_2bapbpy (RCC-bapbpy, R = trimethylsilyl) in ethanol led to the formation of various side products, e.g. ^{1}H NMR analysis showed the formation of enol esters.

5.1 Introduction

NAMI-A and KP1019 represent two milestones in the development of ruthenium-based anticancer compounds. Both complexes entered clinical trials and showed promising results.[1, 2] They were studied extensively to understand their chemical and biological properties, as well as their anticancer mode of action.[3, 4] However, for both complexes clinical trials ended without success and therefore the search for other ruthenium-based anticancer drugs continues. A promising new family of anticancer drug candidates is based on ruthenium complexes that can be activated by visible light. Those phototherapeutic agents are based on either bidentate, tridentate, or tetradentate ligands. The largest family of polypyridyl complexes is based on bidentate ligands, mostly of the 2,2′-bipyridine (bpy) family. Glazer, Salassa, Gasser, and McFarland for example have reported many new complexes of this kind,[5-8] while Turro and Bonnet, among others, developed complexes based on derivatives of the tridentate ligand 2,2′:6′,2″-terpyridine (tpy).[9-13] Finally, tetradentate pyridyl ligands have also been used to synthesize ruthenium compounds.[14-17] One promising example of such a tetrapyridyl ligand is N6,N6'-di(pyridine-2-yl)-2,2'-bipyridine-6,6'-diamine (H_2bapbpy) and its derivatives. Many ruthenium(II) complexes compromising these ligands are light-activatable, but non-emissive and thus cannot be monitored in cells by microscopy to study their intracellular distribution. For such complexes, referred to as photoactivated chemotherapy agents, alkyne functionalization, followed by post-treatment click chemistry with an azido-functionalized fluorophore, is one of the few methods available to monitor their distribution in cells.

Here, we report the synthesis of alkyne-functionalized ruthenium complexes using the synthesis method developed in Chapter 2. The alkyne handle allows fluorophore labeling *via* a CuAAC reaction to investigate the cellular distribution and mode of action of the complexes. Three ruthenium compounds were investigated (Figure 5.1): [Ru(tpy)(bpy)(MTI-SRR′)]$(PF_6)_2$ ([**1**]$(PF_6)_2$) where MTI-SRR′ is a thioether-rigidin conjugate. The rigidin derivative is known to cause cell death through impeding microtubule function,[18] while the thioether moiety allows the coordination of the rigidin to ruthenium. The ruthenium complex is non-toxic and "cages" the rigidin toxin in the dark.[19] The toxicity after light activation is hence due to the photoreleased ligand. In contrast, the tris-heteroleptic ruthenium complex [Ru(Ph_2phen)(mtmp)(bpy)]$(PF_6)_2$ ([**2**]$(PF_6)_2$), where Ph_2phen = 4,7-diphenyl-1,10-phenantroline, and mtmp = 2-(methylthio)methylpyridine, is a

photoactivated chemotherapy compound where phototoxicity comes from the metal center. The combination of spectator ligands provides an excellent balance between lipophilicity and photosubstitution.[20] In this complex, light irradiation releases the non-toxic N,S ligand mtmp and the cytotoxic aqua ruthenium complex. Alkyne functionalization of the ancillary 2,2′-bipyridine ligand would allow for tracing of the toxic aqua complex within a cell. Finally, [Ru(H_2bapbpy)(DMSO)(Cl)]Cl ([**3**]Cl), is a tetrapyridyl ruthenium complex that is cytotoxic due to the photogenerated *trans*-[Ru(H_2bapbpy)(OH_2)]$^{2+}$ species.[15] Alkyne functionalization of the H_2bapbpy ligand is performed on its non-coordinated amine bridges,[14] which are in principle easier to functionalize than the pyridyl rings.

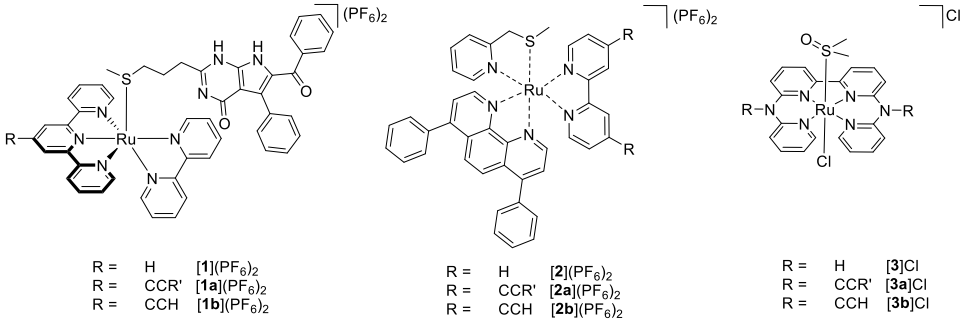

Figure 5.1. Schematic structures of the complexes [**1**](PF_6)$_2$, [**2**](PF_6)$_2$, and [**3**]Cl, described in this Chapter. For [**1a**](PF_6)$_2$ and [**2a**](PF_6)$_2$, R′ = *tert*-butyldimethylsilyl, for complex [**3a**]Cl, R′= trimethylsilyl. For complex [**2**](PF_6)$_2$, two isomers are formed, which are not specified here.

5.2 Results and Discussion

5.2.1 Alkyne functionalization of a tpy-based PACT complex

For the alkyne functionalization of the complex [**1**](PF_6)$_2$, the tpy ligand was modified as described in Chapter 2. Coordination of RCC-tpy (where R = *tert*-butyldimethylsilyl) to ruthenium(III) precursor $RuCl_3$, followed by reaction with bpy resulted in the chloride complex [Ru(RCC-tpy)(bpy)(Cl)]Cl ([**4**]Cl). Attempts to synthesize [Ru(RCC-tpy)(bpy)(MTI-SRR′)](PF_6)$_2$ ([**1a**](PF_6)$_2$) according to the known reaction procedure *via* the aqua complex [Ru(RCC-tpy)(bpy)(OH_2)]$^{2+}$ ([**5**]$^{2+}$) failed due to the hydrophobicity of the MTI-SRR′ ligand: the addition of water is necessary to drive the hydrolysis of the chloride ligand and to produce some aqua complex [**5**]$^{2+}$ in solution, but it also results in precipitation of the MTI-SRR′ ligand. In addition, the ligand is non-commercial and cannot be added in large excess to the reaction mixture to drive the reaction to completion, as was done with

2-(methylthio)ethanol in Chapter 2. A new synthetic route was hence developed, *via* the acetonitrile intermediate [Ru(RCC-tpy)(bpy)(MeCN)]$(PF_6)_2$ ([**6**]$(PF_6)_2$). [**6**]$(PF_6)_2$ was obtained by white light irradiation of [**4**]Cl in acetonitrile for 22 h. It was expected that the acetonitrile ligand, in contrast to a labile water ligand, protects the coordination sphere of the metal ion from alkyne reactivity. For [**1**]$(PF_6)_2$, coordination of the MTI-SRR' ligand took place in ethylene glycol at 100 °C. Knowing from previous reactions that the reaction temperature in presence of the alkyne group should be lower than 80 °C, [**1a**]$(PF_6)_2$ was synthesized by coordination of MTI-SRR' to [**6**]$(PF_6)_2$ at 70 °C and the reaction time was extended to 7 d (Scheme 5.1). Precipitation yielded an off-white solid with peaks in the MS spectrum at m/z = 334.7, 516.3, and 330.6, indicating that the reaction product is a mixture of starting material [**6**]$(PF_6)_2$ (calc. m/z = 335.1, $[Ru(RCC\text{-}tpy)(bpy)(MeCN)]^{2+}$) and the desired complex [**1a**]$(PF_6)_2$ (calc. m/z = 516.2, $[Ru(RCC\text{-}tpy)(bpy)(MTI\text{-}SRR')]^{2+}$) and a third species. ^{1}H NMR analysis confirmed the presence of [**6**]$(PF_6)_2$ and [**1a**]$(PF_6)_2$ with their characteristic A6 peaks at 9.75 and 9.71 ppm in methanol-d_4 and showed the signal of the third species at 9.57 ppm. This signal might belong to either the aqua species $[\mathbf{5}]^{2+}$ or the methanol complex $[Ru(RCC\text{-}tpy)(bpy)(MeOH)]^{2+}$ (calc. m/z = 330.6). Separation of the complexes by size exclusion column chromatography was not successful, as the complex mixture was unstable under these conditions. Thus, so far, the complex was isolated as 2:1:2 ratio mixture of [**1a**]$(PF_6)_2$: [**6**]$(PF_6)_2$: unknown side product (Figure 5.2). The deprotection of the alkyne group with potassium fluoride to obtain [**1b**]$(PF_6)_2$ was not attempted on the complex mixture. Overall, the acetonitrile complex offers an alternative starting point for coordination reaction with hydrophobic ligands that cannot be added in excess, but driving the coordination reaction to completion without increasing the temperature above 80 °C remains a challenge.

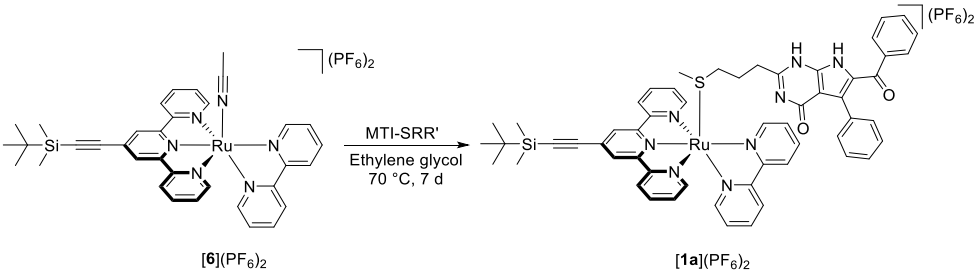

[**6**]$(PF_6)_2$ [**1a**]$(PF_6)_2$

Scheme 5.1. Reaction scheme of the synthesis of the alkyne-functionalized complex [**1a**]$(PF_6)_2$.

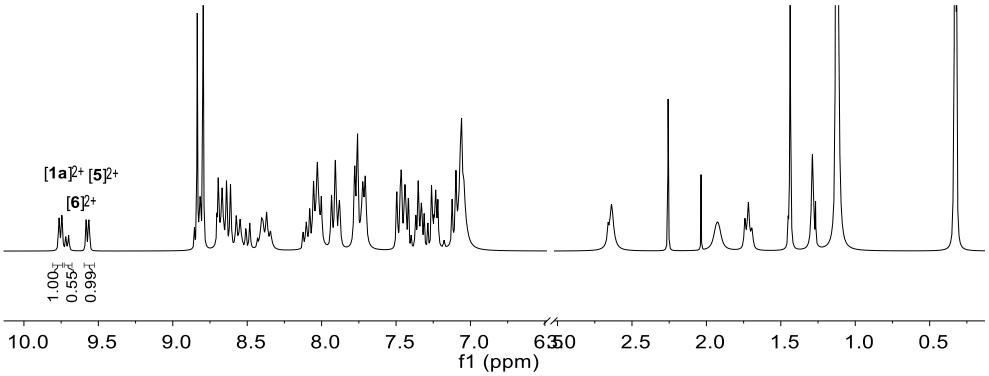

Figure 5.2 ^{1}H NMR spectrum of a solution of the product mixture in methanol-d_4 of the reaction between [**6**]$(PF_6)_2$ and MTI-SRR'.

5.2.2 Alkyne functionalization of a bpy-based PACT complex

Alkyne functionalization of the bpy ligand is well-reported in literature with trimethylsilyl (TMS) as protecting group.[21, 22] Here, *tert*-butyldimethylsilyl (TBDMS, R) was used. 4,4'-Bis(*tert*-butyldimethylsilylethynyl)-2,2'-bipyridine (RCC-bpy) was synthesized from 4,4'-dibromo-2,2'-bipyridine and *tert*-butyldimethylsilylethyne in a 1:18 ratio in triethylamine (TEA) (Scheme 5.2), followed by purification on a silica column. The MS spectrum of the product showed signals at m/z = 433.6 corresponding to (RCC-bpy + H)$^+$ (calc. m/z = 433.3), and the ^{1}H NMR spectrum in chloroform-d shows the characteristic relative ratio (9:6) of the *tert*-butyl protons to the protons of the two dimethyl groups of the protecting R group at 1.00 and 0.20 ppm, respectively.

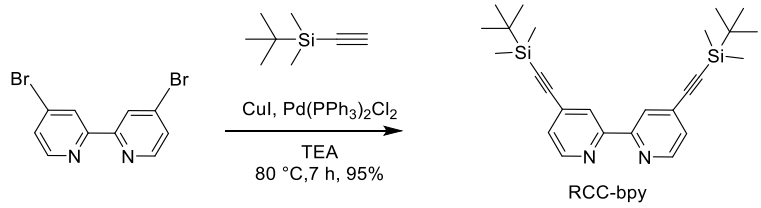

Scheme 5.2. Reaction scheme of the synthesis of the alkyne-functionalized RCC-bpy ligand.

The known acetonitrile precursor [Ru(Ph$_2$phen)(mtmp)(MeCN)$_2$](ClO$_4$)$_2$ ([**7**](ClO$_4$)$_2$) was reacted with the RCC-bpy ligand to obtain the heteroleptic light-activatable ruthenium complex [Ru(Ph$_2$phen)(mtmp)(RCC-bpy)](PF$_6$)$_2$ ([**2a**](PF$_6$)$_2$, Scheme 5.3).[20, 23] Here again, the acetonitrile groups of the precursor complex [**7**]$^{2+}$ prevented the reaction of the alkynes with the ruthenium center. For the synthesis of [**2a**](PF$_6$)$_2$, the presence of these acetonitrile groups is even more important

because of the increased number of free coordination sites compared to precursors such as [**6**]$^{2+}$. The formation of additional side products is known for ruthenium complexes with two available coordination sites in *cis*-position.[21] The reaction conditions used for the synthesis of the non-functionalized complex [**2**]$(PF_6)_2$ had to be adapted for the presence of the alkynes: instead of ethylene glycol, the reaction was performed in methanol at reflux temperature (70 °C) for 7 d (experimentally determined by NMR experiments, Figure AV.1). After precipitation with aqueous potassium hexafluoridophosphate solution, MS analysis (m/z = 502.6; calc. m/z = 502.7 for [Ru(Ph$_2$phen)(mtmp)(RCC-bpy)]$^{2+}$) and ^{1}H NMR spectroscopy in chloroform-d (Figure 5.3) confirmed the formation of the desired complex [**2a**]$(PF_6)_2$. The complex was isolated as a mixture of configuration isomers, like for [**2**]$(PF_6)_2$.[20] Removal of the TBDMS protecting group was attempted with five equivalents of potassium fluoride in methanol overnight at 30 °C. A decrease of the ^{1}H NMR peaks in methanol-d$_6$ belonging to the protecting group (1.04 and 0.24 ppm) and the appearance of new singlet peaks at 4.61 and 4.47 ppm for the free alkynes of both isomers indicated that partial deprotection of the terminal alkynes had occurred. However, full deprotection and isolation of pure [**2b**]$(PF_6)_2$ was not achieved.

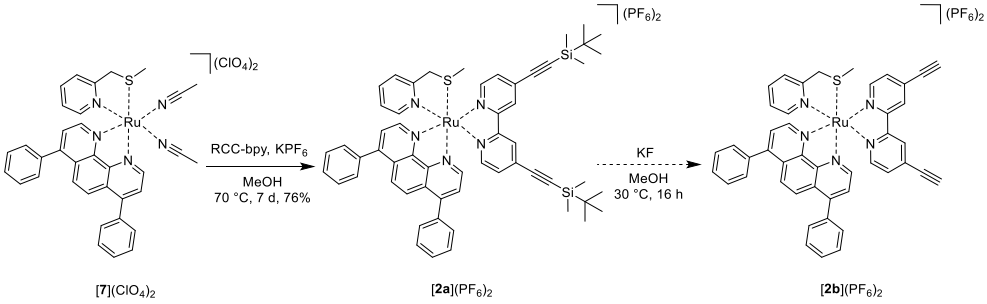

Scheme 5.3. Reaction scheme of the synthesis of the alkyne-functionalized complex [**2a**]$(PF_6)_2$.

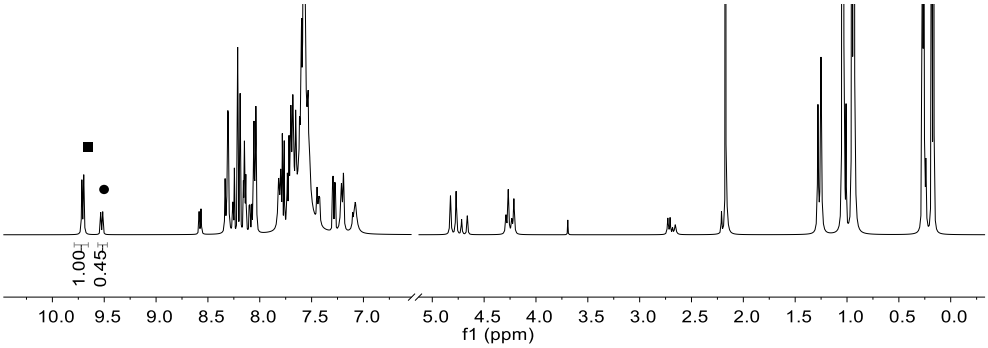

Figure 5.3 ^{1}H NMR spectrum of a solution of [**2a**]$(PF_6)_2$ in chloroform-d. Signals indicated with black square (■) and circle (●) correspond to the two isomers of complex [**2a**]$(PF_6)_2$.

5.2.3 Alkyne-functionalized bapbpy-based ruthenium complex

The tetradentate ligand H_2bapbpy was functionalized on both non-coordinating amine bridges. The alkyne-functionalized RCC-bapbpy ligand (R = trimethylsilyl, Scheme 5.4) was synthesized by the reaction of H_2bapbpy and commercially available 3-(trimethylsilyl)propargyl bromide in the presence of sodium hydride in DMF for 3 h at 0 °C, as TBDMS-protected propargyl bromide is not commercially available. After extraction with ethyl acetate, evaporation, and washing with methanol, RCC-bapbpy was isolated in a yield of 17%. The nature of the ligand was confirmed by mass spectrometry (m/z = 561.5; calc. m/z = 561.3 for $(\text{RCC-bapbpy} + H)^+$) and ^{1}H NMR spectroscopy (Figure 5.4). Coordination of RCC-bapbpy to the ruthenium precursor $[Ru(DMSO)_4(Cl)_2]$ was then studied in NMR experiments in deuterated ethanol-d_6 over several hours at 60 °C (Figure and Scheme 5.4). The signals of the free ligand decreased, and new signals appeared in the aromatic as well as in the aliphatic region. The number of new signals indicated that the reaction yielded a mixture of products.

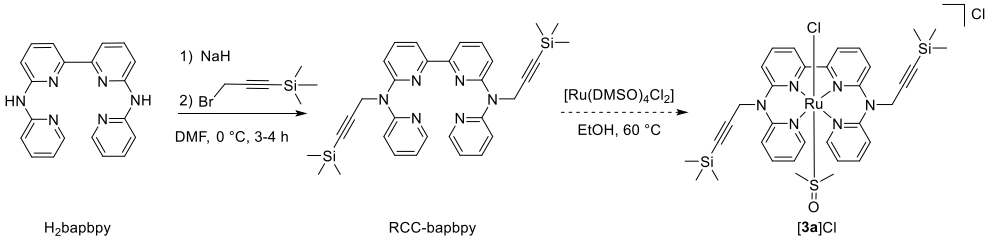

Scheme 5.4. Reaction scheme of the synthesis of the functionalized ligand RCC-bapbpy and its coordination to ruthenium to obtain [**3a**]Cl.

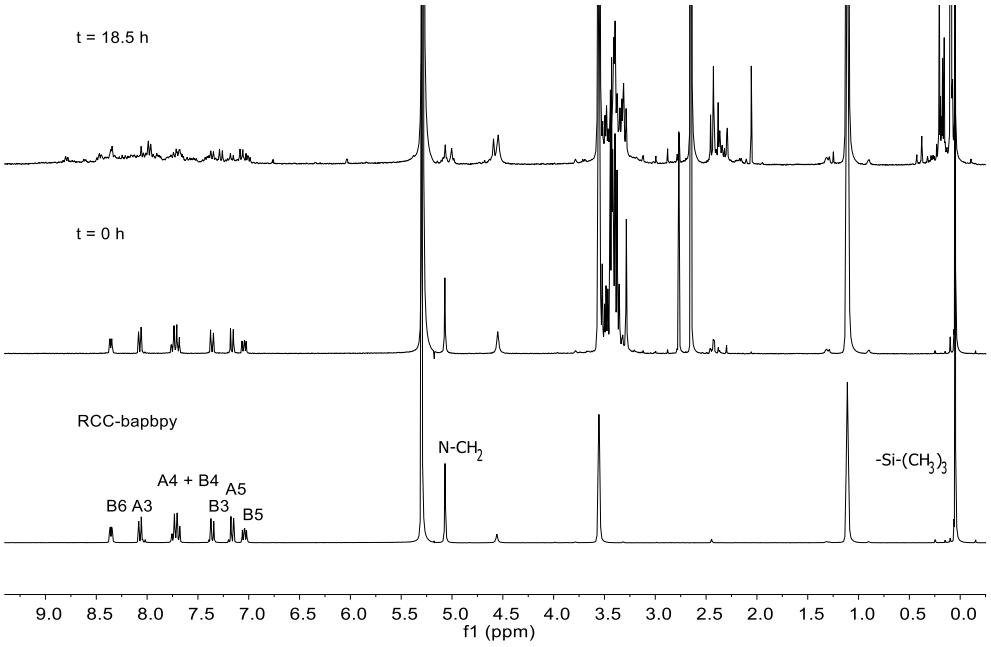

Figure 5.4. ^{1}H NMR evolution of the reaction of [Ru(DMSO)$_4$(Cl)$_2$] and RCC-bapbpy in ethanol-d$_6$ at 60 °C.

To identify the nature of these products, several control experiments were conducted. The thermal stability of the RCC-bapbpy ligand under the reaction conditions was monitored by ^{1}H NMR spectroscopy in deuterated ethanol-d$_6$ in absence of a metal precursor for several days at 60 °C (Figure AV.3). The ^{1}H NMR spectra did show the appearance of new signals while the peaks belonging to the starting ligand disappeared, indicating that the ligand is not stable in solution. When stored at room temperature in solution, the NMR spectrum showed signals belonging to the RCC-ligand, the product seen after heating the ligand at 60 °C, and additional peaks (Figure AV.3). Noteworthy, upon functionalization of the bidentate ligand N,N-dipyridylamine (Hdpa), which represents one half of H$_2$bapbpy, with the same alkyne handle, an unexpected intramolecular rearrangement took place at room temperature (Scheme AV.2 and Figure AV.4). It cannot be excluded that such an intramolecular rearrangement will take place for RCC-bapbpy (Scheme 5.5a). The NMR reaction of [Ru(DMSO)$_4$(Cl)$_2$] in deuterated ethanol-d$_6$ was also performed with the non-protected HCC-bapbpy ligand. After 1 h at 60 °C, the signals of the starting materials disappeared and very broad, ill-defined signals appeared (Figure AV.5). A dark insoluble precipitate was formed that could not be analyzed by NMR spectroscopy or mass spectrometry. Polymerization might have taken place here.[24] When working with the protected RCC-bapbpy ligand, the solution stayed clear

without precipitate formation for the entire time of the experiment (18.5 h). Therefore, polymerization can be excluded as possible side reaction when working with TMS-protected alkynes. In Chapter 2, the formation of an enol ester was reported as side reaction when functionalizing tpy with an alkyne group (Scheme AII.1). Thus, the reaction of $[Ru(DMSO)_4(Cl)_2]$ and RCC-bapbpy was repeated in non-deuterated ethanol to investigate possible side reactions involving ethanol. The aromatic regions of the ^1H NMR spectra of the reaction mixtures obtained in deuterated ethanol-d_6 and non-deuterated ethanol showed similar signals, but in the aliphatic region additional signals at 4.05, 3.59, and 1.16 ppm were found (Figure 5.5) when working in non-deuterated solvent. The fact that these signals were not visible when the reaction was performed in deuterated ethanol-d_6 confirmed that these peaks are the result of a side reaction with ethanol (Scheme 5.5b). The signals are indeed characteristic for an enol ester (Figure AV.6). Repeating the reaction in a non-alcoholic solvent should prevent enol ester formation. Whether this side reaction occurs on both sides of the bapbpy ligand and whether coordination of this new ligand to the ruthenium precursor is possible remained unclear since the MS spectrum of the reaction mixture did not give conclusive results (Figure AV.7). Overall, the functionalization of the amine bridges of H_2bapbpy is not a viable strategy since several side reactions may occur in parallel, and alternative positions of the alkyne groups on the tetradentate ligand should be considered. In addition, the TMS protecting group is not fully protecting the alkyne groups, and a better protecting group should be used (TBDMS).

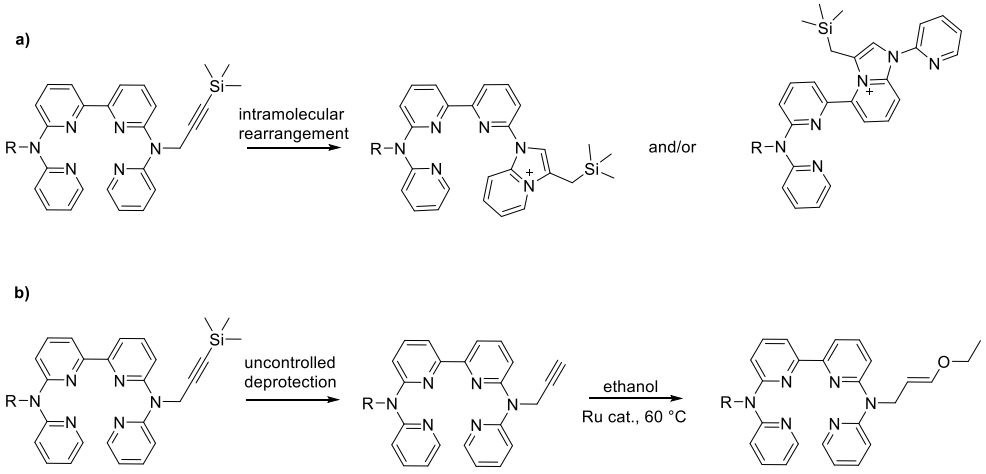

Scheme 5.5. Overview of possible side products in the reaction of RCC-bapbpy with $[Ru(DMSO)_4(Cl)_2]$ in ethanol: a) intramolecular rearrangement of the RCC-bapbpy ligand, and b) enol ester formation after

deprotection of the alkyne groups. The ruthenium(II) species can act as catalyst, and/or coordinate to the new ligands.

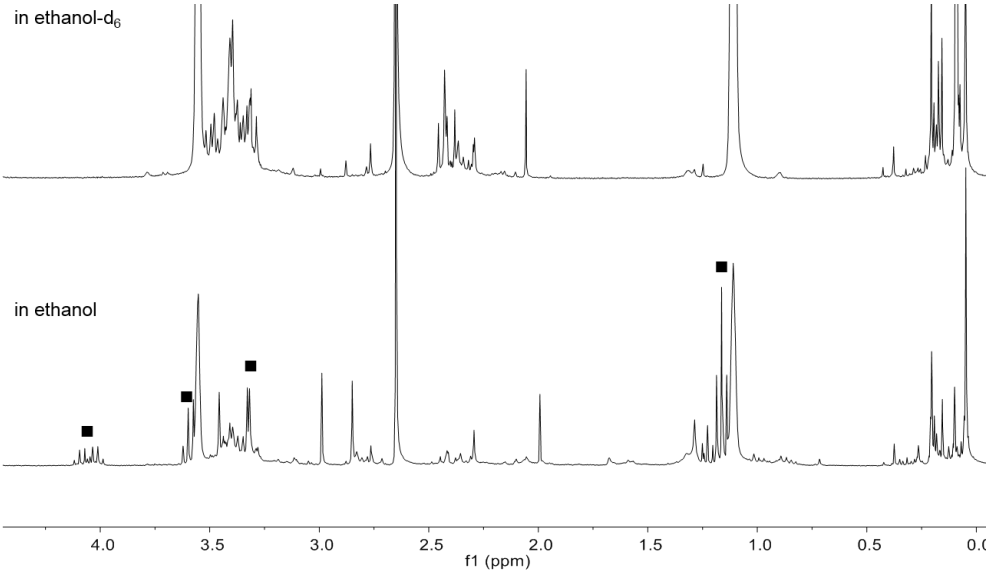

Figure 5.5. ^{1}H NMR spectrum (aliphatic region) of a solution of the reaction product of the reaction between RCC-bapbpy and $[Ru(DMSO)_4(Cl)_2]$ in ethanol-d_6 or ethanol. The ^{1}H NMR is taken in ethanol-d_6. Signals indicated with black squares (■) correspond to enol esters.

5.3 Conclusion

In conclusion, two polypyridyl ligands were functionalized with short alkyne handles showing that the series of functionalized ligands can easily be extended. The alkyne handle always needs protection during metal coordination to prevent the formation of side products in the following complexation steps. It is necessary to adapt the conditions of the coordination reaction of the functionalized ligand to the instability of the alkyne protecting group. There is not one universal method for all complexation reactions, but specific strategies for each target ruthenium complex have to be found. Those adjustments require effort and time and the optimal conditions are not always easy to predict.

5.4 Experimental

5.4.1 Materials and Methods

(S)-2,2′-Bis(diphenylphosphino)-1,1′-binaphthalene ((S)-BINAP), potassium *tert*-butoxide (KOtBu), bis(dibenzylideneacetone)palladium(0) ($Pd(dba)_2$), 2-amino-4-chloropyridine, p-toluenesulfonic anhydride (Ts_2O), trifluorotoluene ($PhCF_3$), 6-bromo-2,2′-bipyridine, racemic BINAP, 3-bromo-1-(trimethylsilyl)-1-propyne, sodium hydride (NaH) (60% in mineral oil), triethylamine (Et_3N),

sodium oxalate ($Na_2C_2O_4$), and potassium hexafluoridophosphate (KPF_6) were purchased form Sigma Aldrich; 6,6′-dibromo-2,2′-bipyridine from Tokyo Chemical Industry; trifluoroacetic acid and 2,2′-bipyridine from Alpha Aesar; bis(triphenylphosphine)palladium(II) dichloride ($PdCl_2(PPh_3)_2$), tert-butylamine and copper iodide (CuI) from Acros Organics; *tert*-butyldimethylsilylethyne, dipyridylamine (Hdpa), and 4,7-diphenyl-1,10-phenanthroline from ABCR; 4,4′-dibromo-2,2′-bipyridine, and $Pd(PPh_3)_2Cl_2$ from Fischer Scientific. 2-[(Methylthio)methyl] pyridine, *cis*-$RuCl_2(dimethylsulfoxide)_4$, [Ru(RCC-tpy)(bpy)(Cl)]Cl, H_2bapbpy, and microtubule polymerization inhibitor (MTI-SRR′) were synthesized according to literature.[18, 25-28] All syntheses were completed under dinitrogen atmosphere unless otherwise noted and, apart from 4,4′-bis(*tert*-butyldimethylsilylethynyl)-2,2′-bipyridine and $[Ru(RCC\text{-}tpy)(bpy)(MeCN)](PF_6)_2$, under dim light. Et_3N and DMF were dried over molecular sieves (4 Å). All reagents were used without further purification.

NMR spectra were recorded on an AV-300 Bruker spectrometer with chemical shifts indicated in ppm. Mass spectra were recorded on a Thermo Scientific Dionex UltiMate 3000 system. A LOT 1000 W Xenon Arc lamp with an IR short pass filter and a 400 nm long pass filter from Andover Corporation was used for the preparative scale photoreaction.

5.4.2 Synthesis

Synthesis of $[Ru(RCC\text{-}tpy)(bpy)(MeCN)](PF_6)_2$, (R = TBDMS), [6]$(PF_6)_2$

[Ru(RCC-tpy)(bpy)(Cl)]Cl (21 mg, 0.029 mmol) was dissolved in a mixture of acetonitrile/water (100 mL, 3:1 ratio) under air atmosphere in a 100 mL photoreactor (diameter = 5.0 cm, depth = 5.5 cm) placed 7 cm from the focusing lens. This mixture was stirred with a magnetic stirrer and kept at 25 °C with a water-cooling system and irradiated at 800 W with a LOT 1000 W Xenon Arc lamp fitted with IR short pass and 400 nm long pass filters from Andover Corporation. Irradiation was done for periods of 4 to 7 h over 4 d for a total of 22 h. During this time the solution changed from pink-purple to red-orange. The reaction was followed by TLC on silica using a mobile phase of acetone/water/KPF_6 (16:4:1). R_f values for [Ru(RCC-tpy)(bpy)(Cl)]Cl and [**5**]$(PF_6)_2$ are 0.75 and 0.55, respectively. The mixture was added to a stirred saturated aqueous potassium hexafluoridophosphate solution, chilled overnight in the fridge, filtered, and washed with water. [**6**]$(PF_6)_2$ was obtained as dark orange powder in a yield of 50% (6.0 mg, 7.7 μmol).

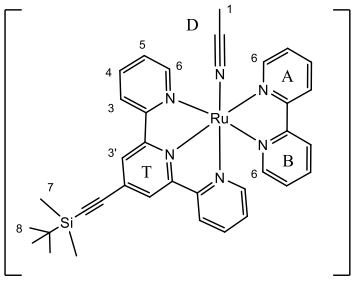

^{1}H NMR (300 MHz, methanol-d_4, 298 K) δ 9.71 (d, *J* = 5.6 Hz, 1H, A6), 8.81 (d, *J* = 8.0 Hz, 1H, A3), 8.81 (s, 2H, T3′), 8.68 (d, *J* = 8.2 Hz, 2H, T3), 8.55 (d, *J* = 8.1 Hz, 1H, B3), 8.40 (t, *J* = 7.4 Hz, 1H, A4), 8.06 (td, *J* = 7.9, 2.2 Hz, 3H, T4 + A5), 7.94 – 7.82 (m, 1H, B4), 7.77 (d, *J* = 5.3 Hz, 2H, T6), 7.50 – 7.37 (m, 3H, T5 + B6), 7.23 – 7.13 (m, 1H, B5), 2.26 (s, 3H, D1), 1.12 (s, 9H, T8), 0.33 (s, 6H, T7). *^{13}C NMR (75 MHz, acetonitrile-d_3, 298 K)* δ 153.0, 152.3, 150.9, 138.8, 137.7, 137.4, 128.3, 127.7, 126.6, 125.3, 124.5, 124.2, 123.7, 25.5. *ES MS m/z (calc.):* 334.7 (335.1 $[M - 2PF_6]^{2+}$).

Synthesis of $[Ru(RCC\text{-}tpy)(bpy)(MTI\text{-}SRR')](PF_6)_2$, (R = TBDMS), [1a]$(PF_6)_2$

$[Ru(RCC\text{-}tpy)(bpy)(MeCN)](PF_6)_2$ (9.0 mg, 9.4 μmol) and MTI-SRR′ (3.8 mg, 9.4 μmol) were dissolved in ethylene glycol (3 mL) and heated for 7 d at 70 °C. The reaction was followed by silica gel TLC on Al foil

plates (16:4:1 acetone/water/KPF_6, R_f = 0.69). After cooling to room temperature, the solution was added to a saturated aqueous solution of potassium hexafluoridophosphate (40 g/L) and chilled in the fridge overnight. Then, the orange precipitate was collected on a Millipore filter and washed with water and diethyl ether (3 x 10 mL each). The complex was then re-dissolved in acetone (20 mL) and added to saturated aqueous potassium hexafluoridophosphate solution (40 g/L, 20 mL). A rotary evaporator was used to remove acetone until the complex precipitated, at which point it was filtered and washed again with water and diethyl ether (3 x 10 mL each). A dark red solid was obtained (8.0 mg).

The ^{1}H NMR spectrum showed a mixture of [**1a**]$(PF_6)_2$: [**6**]$(PF_6)_2$: unknown byproduct in a ratio 2:1:2. *ESI-MS m/z (calc.):* 330.6, (330.6, [Ru(RCC-tpy)(bpy)(MeOH)]$^{2+}$), 334.7, (335.1, [Ru(RCC-tpy)(bpy)(MeCN)]$^{2+}$), 516.3 (516.2, [Ru(RCC-tpy)(bpy)(MTI-SRR')]$^{2+}$).

Synthesis of 4,4′-bis(*tert-b*utyldimethylsilylethynyl)-2,2′-bipyridine, RCC-bpy (R = TBDMS)

4,4′-Bis(*tert-b*utyldimethylsilylethynyl)-2,2′-bipyridine was synthesized according to a modified literature procedure.[1] Under dry conditions, 4,4′-dibromo-2,2′-bipyridine (250 mg, 0.80 mmol), CuI (19 mg, 0.10 mmol), $Pd(PPh_3)_2Cl_2$ (35 mg, 0.050 mmol), and *tert*-butyldimethylsilylethyne (0.90 mL, 4.8 mmol) were added to triethylamine (4 mL) and refluxed for 7 h at 80 °C. During the reflux, the same amounts of triethylamine and *tert*-butyldimethylsilylethyne were added twice (after 2 h 20 min and 4 h 40 min). After 7 h, the solvents were evaporated, the solid was dissolved in n-hexane, and filtered. The filtrate was purified by silica column with hexane/ethyl acetate (8:2) as eluent (R_f = 0.83). Yield: 95% (327 mg, 0.757 mmol).

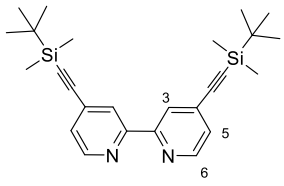

^{1}H NMR (300 MHz, chloroform-d, 298 K) δ 8.62 (dd, *J* = 5.0, 0.9 Hz, 2H, 6), 8.42 (dd, *J* = 1.6, 0.9 Hz, 2H, 3), 7.33 (dd, *J* = 5.0, 1.6 Hz, 2H, 5), 1.00 (s, 18H, -Si-C(CH_3)$_3$), 0.20 (s, 12H, -Si-(CH_3)$_2$). *^{13}C NMR (75 MHz, chloroform-d, 298 K)* δ 155.7 (2), 149.2 (6), 132.5 (4), 126.1 (5), 123.6 (3), 103.0 (-C$\underline{C}$-Si), 98.6 (-$\underline{C}$C-Si), 26.2 (-Si-C($\underline{C}H_3$)$_3$), 16.8 (-Si-$\underline{C}$(CH_3)$_3$), −4.6 (-Si-($\underline{C}H_3$)$_2$). *ES MS m/z (calc.):* 433.6 (433.3, [M + H]$^+$).

Synthesis of [Ru(Ph$_2$phen)(mtmp)(RCC-bpy)](PF$_6$)$_2$, [2a](PF$_6$)$_2$ (R = TBDMS)

$[Ru(Ph_2phen)(mtmp)(MeCN)_2](ClO_4)_2$ (10.0 mg, 0.0117 mmol) and 4,4′-bis(*tert*-butyldimethylsilylethynyl)-2,2′-bipyridine (5.0 mg, 0.012 mmol) were dissolved in methanol (3 mL). The mixture was heated for 7 d at 70 °C. After cooling to room temperature, the bright red-orange mixture was added to a stirred, saturated aqueous solution of potassium hexafluoridophosphate (40 g/L) and chilled in the fridge overnight. The precipitate was filtered and washed with water and diethyl ether. [**2a**]$(PF_6)_2$ was obtained in a yield of 76% (9 mg, 9 μmol) as a mixture of two coordination isomers in a 0.45:1 ratio.

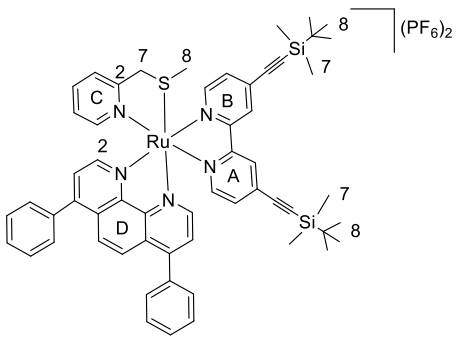

^{1}H NMR (300 MHz, chloroform-d, 298 K) δ 9.71 (d, *J* = 5.5 Hz), 9.52 (d, *J* = 5.9 Hz), 8.36 – 7.99 (m), 7.84 – 7.41 (m), 7.28 (dd, *J* = 5.9, 1.7 Hz), 7.20 (d, *J* = 5.8 Hz), 7.09 (d, *J* = 7.6 Hz), 5.30 (s), 4.80 (d, *J* = 16.3 Hz), 4.69 (d, *J* = 16.5 Hz), 4.25 (dd, *J* = 16.5, 6.5 Hz), 3.49 (s), 2.17 (s), 1.27 (d, *J* = 8.7 Hz), 1.04 (s), 1.03 (s), 0.95 (s), 0.94 (s), 0.27 (s), 0.26 (s), 0.18 (s), 0.17 (s). *^{13}C NMR (75 MHz, chloroform-d, 298 K)* δ 156.6, 150.3, 150.3, 135.2, 135.1, 133.9, 133.1, 129.3, 129.0, 77.4, 77.0, 76.6. *ESI-MS m/z (calc.):* 502.6 (502.7, $[M - 2PF_6]^{2+}$).

Synthesis of RCC-bapbpy, (R = TMS)

The reaction was performed under anhydrous conditions. Sodium hydride (52 mg, 1.3 mmol) was added portion wise to a solution of H_2bapbpy (100 mg, 0.29 mmol) in DMF (1.7 mL) at 0 °C. The reaction mixture was stirred at 0 °C for 30 min and 3-(trimethylsilyl)propargyl bromide (1.1 mL, 6.5 mmol) was added dropwise. The mixture was stirred at 0 °C for 3 h. Then, water (60 ml) was added and the mixture was extracted with ethyl acetate (4 × 25 mL). The combined organic layers were dried over sodium sulfate, filtered and concentrated. The residue was purified by chromatography over silica gel (gradient from 100% dichloromethane to 95:5 dichloromethane/methanol). The product fractions were collected, and the solvent was evaporated. The RCC-bapbpy was obtained in a yield of 17% (28 mg, 0.05 mmol).

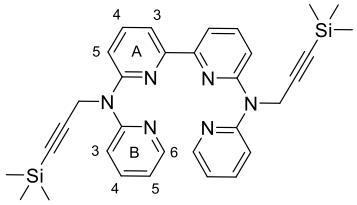

^{1}H NMR (300 MHz, DMSO-d$_6$, 298 K) δ 8.38 (ddd, *J* = 5.0, 2.0, 0.8 Hz, 2H, B6), 7.98 (d, *J* = 7.5 Hz, 2H, A3), 7.88 – 7.76 (m, 2H, A4), 7.79 – 7.71 (m, 2H, B4), 7.36 (dt, *J* = 8.4, 1.0 Hz, 2H, B3), 7.27 (d, *J* = 8.2 Hz, 2H, A5), 7.06 (ddd, *J* = 7.3, 4.8, 0.9 Hz, 2H, B5), 5.06 (s, 4H, N-C$\underline{H}_2$-), 0.05 (s, 18H, -Si(C$\underline{H}_3$)$_3$). *^{13}C NMR (75 MHz, DMSO-d$_6$, 298 K)* δ 155.6 + 154.9 + 153.5 (A2 + A6 + B2), 148.0 (B6), 138.5 (A4), 137.9 (B4), 118.1 (B5), 114.9 (B3), 114.2 (A5), 114.0 (A3), 104.0 (CH$_2$-$\underline{C}$C-), 86.5 (-C$\underline{C}$-Si), 38.1 (N-$\underline{C}$H$_2$-), -0.1 (-Si($\underline{C}$H$_3$)$_3$). *ES MS m/z (calc.):* 561.5 (561.3, $[M + H]^+$).

Attempted synthesis of [Ru(RCC-bapbpy)(DMSO)(Cl)]Cl

[Ru(DMSO)$_4$(Cl)$_2$] (2.5 mg, 5.1 μmol) and RCC-bapbpy (2.3 mg, 4.1 μmol) were dissolved in deuterated ethanol-d$_6$ (0.5 mL) under dinitrogen atmosphere in an NMR tube with PFTE stopper. The reaction mixture was heated at 60 °C in the NMR tube. ^{1}H NMR spectra of the reaction were recorded at different reaction times.

[Ru(DMSO)$_4$(Cl)$_2$] (10.4 mg, 0.021 mmol) and RCC-bapbpy (10.0 mg, 0.018 mmol) were dissolved in ethanol (5 mL) under dinitrogen atmosphere. The reaction mixture was heated at 60 °C while stirring for 18.5 h. The solvent was evaporated, and the reaction mixture was analyzed by MS and ^{1}H NMR analysis.

5.4.3 Supporting Information

The synthetic routes for the synthesis of HCC-dpa and HCC-bapbpy are reported. ^{1}H NMR spectra of the synthesis of [**2a**](PF$_6$)$_2$ and of stability measurements of RCC-bapbpy, as well as the characterization of the HCC-bapbpy intramolecular rearrangement product are provided in Appendix IV.

5.5 Contribution

Emma Cleary and Dr. Sipeng Zheng helped to synthesize some of the ligands and ruthenium complexes. Dr. Sylvestre Bonnet and Prof. Lies Bouwman provided experimental guidance and significant editorial feedback.

5.6 References

1 C. G. Hartinger, S. Zorbas-Seifried, M. A. Jakupec, B. Kynast, H. Zorbas, and B. K. Keppler, *J. Inorg. Biochem.* **2006**, 100 (5), 891-904.

2 E. Alessio, *Eur. J. Inorg. Chem.* **2017**, 2017 (12), 1549-1560.

3 J. Malina, O. Novakova, B. K. Keppler, E. Alessio, and V. Brabec, *J. Biol. Inorg. Chem.* **2001**, 6 (4), 435-445.

4 C. G. Hartinger, M. A. Jakupec, S. Zorbas-Seifried, M. Groessl, A. Egger, W. Berger, H. Zorbas, P. J. Dyson, and B. K. Keppler, *Chem. Biodiversity* **2008**, 5 (10), 2140-2155.

5 Y. Arenas, S. Monro, G. Shi, A. Mandel, S. McFarland, and L. Lilge, *Photodiagnosis Photodyn. Ther.* **2013**, 10 (4), 615-625.

6 B. S. Howerton, D. K. Heidary, and E. C. Glazer, *J. Am. Chem. Soc.* **2012**, 134 (20), 8324-8327.

7 E. Wachter, D. K. Heidary, B. S. Howerton, S. Parkin, and E. C. Glazer, *Chem. Commun.* **2012**, 48 (77), 9649-9651.

8 C. Mari, V. Pierroz, R. Rubbiani, M. Patra, J. Hess, B. Spingler, L. Oehninger, J. Schur, I. Ott, L. Salassa, S. Ferrari, and G. Gasser, *Chem. Eur. J.* **2014**, 20 (44), 14421-14436.

9 R. E. Goldbach, I. Rodriguez-Garcia, J. H. van Lenthe, M. A. Siegler, and S. Bonnet, *Chem.Eur. J.* **2011**, 17 (36), 9924-9929.

10 B. Siewert, V. H. van Rixel, E. J. van Rooden, S. L. Hopkins, M. J. Moester, F. Ariese, M. A. Siegler, and S. Bonnet, *Chem.Eur. J.* **2016**, 22 (31), 10960-10968.

11 L. N. Lameijer, S. L. Hopkins, T. G. Brevé, S. H. C. Askes, and S. Bonnet, *Chem. Eur. J.* **2016**, 22 (51), 18484-18491.

12 L. M. Loftus, J. K. White, B. A. Albani, L. Kohler, J. J. Kodanko, R. P. Thummel, K. R. Dunbar, and C. Turro, *Chem. Eur. J.* **2016**, 22 (11), 3704-3708.

13 O. Novakova, J. Kasparkova, O. Vrana, P. M. van Vliet, J. Reedijk, and V. Brabec, *Biochemistry* **1995**, 34 (38), 12369-12378.

14 V. H. S. van Rixel, B. Siewert, S. L. Hopkins, S. H. C. Askes, A. Busemann, M. A. Siegler, and S. Bonnet, *Chem. Sci.* **2016**, 7 (8), 4922-4929.

15 V. H. S. van Rixel, G. F. Moolenaar, M. A. Siegler, L. Messori, and S. Bonnet, *Dalton Trans.* **2018**, 47 (2), 507-516.

16 D. Havrylyuk, M. Deshpande, S. Parkin, and E. C. Glazer, *Chem. Commun.* **2018**, 54 (88), 12487-12490.

17 R. Sharma, J. D. Knoll, P. D. Martin, I. Podgorski, C. Turro, and J. J. Kodanko, *Inorg. Chem.* **2014**, 53 (7), 3272-3274.

18 D. C. Medellin, Q. Zhou, R. Scott, R. M. Hill, S. K. Frail, R. Dasari, S. J. Ontiveros, S. C. Pelly, W. A. L. van Otterlo, T. Betancourt, C. B. Shuster, E. Hamel, R. Bai, D. V. LaBarbera, S. Rogelj, L. V. Frolova, and A. Kornienko, *J. Med. Chem.* **2016**, 59 (1), 480-485.

19 V. H. S. Van Rixel, Toward selective anticancer metallodrugs **2017**, Leiden University, Leiden.

20 J.-A. Cuello-Garibo, Caging ruthenium complexes with non-toxic ligands for photoactivated chemotherapy **2017**, Leiden University, Leiden.

21 N. Zabarska, D. Sorsche, F. W. Heinemann, S. Glump, and S. Rau, *Eur. J. Inorg. Chem.* **2015**, 2015 (29), 4869-4877.
22 R. Ziessel, J. Suffert, and M.-T. Youinou, *J. Org. Chem.* **1996**, 61 (19), 6535-6546.
23 C. S. Burke and T. E. Keyes, *RSC Advances* **2016**, 6 (47), 40869-40877.
24 C. Slugovc, D. Doberer, C. Gemel, R. Schmid, K. Kirchner, B. Winkler, and F. Stelzer, *Monatsh. Chem.* **1998**, 129 (3), 221-233.
25 E. Reisner, T. C. Abikoff, and S. J. Lippard, *Inorg. Chem.* **2007**, 46 (24), 10229-10240.
26 J. R. Alston, S. Kobayashi, T. J. Younts, and J. C. Poler, *Polyhedron* **2010**, 29 (13), 2696-2702.
27 J. B. Gerken, M. L. Rigsby, R. E. Ruther, R. J. Pérez-Rodríguez, I. A. Guzei, R. J. Hamers, and S. S. Stahl, *Inorg. Chem.* **2013**, 52 (6), 2796-2798.
28 S. Bonnet, M. A. Siegler, J. S. Costa, G. Molnar, A. Bousseksou, A. L. Spek, P. Gamez, and J. Reedijk, *Chem. Commun.* **2008**, (43), 5619-5621.